AD-A176 124 PROPERTIES OF MATERIALS USING ACOUSTIC WAVES(U) YALE UNIV NEW HAVEN CT DEPT OF MECHANICAL ENGINEERING R E APFEL NOV 86 N00014-85-K-0215 1/1

UNCLASSIFIED F/G 20/1 NL

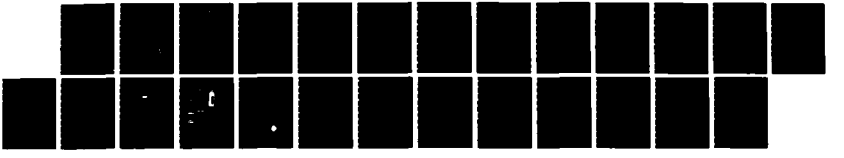

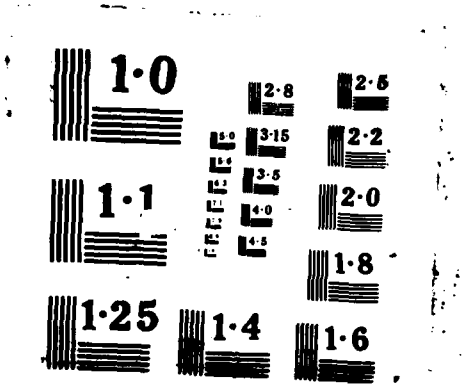
1·0
1·1
1·25
1·4
1·6
1·8
2·0
2·2
2·5
2·8
3·15
3·5
4·0
4·5

(12)

ANNUAL SUMMARY REPORT

PROPERTIES OF MATERIALS USING ACOUSTIC WAVES

supported by the

OFFICE OF NAVAL RESEARCH

under contract

N00014-85-K-0215

for the period

1 February 1986-31 January 1985

to

YALE UNIVERSITY

Principal Investigator: Robert E. Apfel

November 26, 1986

Unclassified

SECURITY CLASSIFICATION OF THIS PAGE (When Data Entered)

REPORT DOCUMENTATION PAGE	READ INSTRUCTIONS BEFORE COMPLETING FORM
1. REPORT NUMBER	2. GOVT ACCESSION NO. AD-A176 124 / 3. RECIPIENT'S CATALOG NUMBER
4. TITLE (and Subtitle) PROPERTIES OF MATERIALS USING ACOUSTIC WAVES	5. TYPE OF REPORT & PERIOD COVERED Annual Summary Nov. 1, 1985-Nov. 1, 1986
	6. PERFORMING ORG. REPORT NUMBER
7. AUTHOR(s) Prof. Robert E. Apfel	8. CONTRACT OR GRANT NUMBER(s) N000014-85-K-0215
9. PERFORMING ORGANIZATION NAME AND ADDRESS Dept. Of Mechanical Engineering, Yale Univ. P.O. Box 2159, 9 Hillhouse, Ave., New Haven CT 06520	10. PROGRAM ELEMENT, PROJECT, TASK AREA & WORK UNIT NUMBERS 61153N (Prog. El. #) RR011-08-01(Proj. Task Area) NR 384-701 (Work Unit #)
11. CONTROLLING OFFICE NAME AND ADDRESS Office Of Naval Research Physics Division Office Arlington, VA 22217	12. REPORT DATE November 1986
	13. NUMBER OF PAGES 22
14. MONITORING AGENCY NAME & ADDRESS(if different from Controlling Office)	15. SECURITY CLASS. (of this report) unclassified
	15a. DECLASSIFICATION DOWNGRADING SCHEDULE
16. DISTRIBUTION STATEMENT (of this Report) Approved for public release; distribution unlimited	Accession For NTIS GRA&I ☑ DTIC TAB ☐ Unannounced ☐ Justification
17. DISTRIBUTION STATEMENT (of the abstract entered in Block 20, if different from Report)	By Distribution/ Availability Codes Dist | Avail and/or Special A-1
18. SUPPLEMENTARY NOTES DTIC COPY INSPECTED 1	

19. KEY WORDS (Continue on reverse side if necessary and identify by block number)

Interfacial characterization; acoustic nonlinear parameter; microparticle characterization; acoustic scattering.

20. ABSTRACT (Continue on reverse side if necessary and identify by block number)

This report summarizes our projects in four areas: 1) Interfacial characterization in the presence of surfactants (theory and experiment); 2) The acoustic nonlinearity parameter: precise measurement and predicting the composition of mixtures; 3) Microparticle characterization using scattering of 30 MHz ultrasonic waves; 4) Stealth acoustics, or how to minimize the signature of objects when the wavelength is comparable to size.

DD FORM 1 JAN 73 1473 EDITION OF 1 NOV 65 IS OBSOLETE

S N 0102-LF-014-6601

Unclassified

SECURITY CLASSIFICATION OF THIS PAGE (When Data Entered)

Table of Contents

I. Progress Report

A. Interfacial Characterization in the Presence of Surfactants: Experiment and Theory

For years researchers have tried to understand phenomena that occur at the fluid-fluid interface. At the end of the last century, Plateau(1) observed the different damping rates of an oscillating compass needle in bulk fluids and at liquid surfaces, and introduced the idea of surface viscosity which was later put on a firmer ground by other workers. It was then accepted in the beginning of this century that, besides the usual bulk fluid properties, viscoelastic properties, surface viscosities and surface elasticity, must be considered in order to explain dissipative aspects of contaminated interfaces. Surface viscosities are the exact analogies of bulk viscosities except that they manifest themselves through the motions at the interface of fluids. Therefore, they add additional dissipation to the system. The surface elasticity, also termed Gibbs elasticity, exists only in multicomponent systems, especially in surfactant solutions. A surfactant is a substance in which each molecule includes two chemical groups that differ greatly in their solubility in a solvent. Because of the different solubilities, they accumulate at the interface. Consequently, the interfacial tension is reduced since the interface is not as energetically unfavorable as that without surfactant molecules.

The first explanation of Gibbs elasticity was given by Gibbs (2) for a flat thick film. It occurs when a film is stretched. The stretching increases the film's surface area, providing new opportunities for surfactant molecules to come to the surface. Nevertheless, the surface tension increases since there are few surfactant molecules per unit area of the surface. Thus, a stretched film will try to contract like an elastic skin. Unfortunately, these properties are not easy to measure. It is because of this that one needs to consider the diffusion and adsorption of surfactants and employ the proper boundary conditions in order to have a complete description of the system. Most of the methods consist of exciting the interface and analyzing the resulting motions to infer the surface properties. For example, L. Ting et al. (3) used longitudinal surface waves to study the dynamic properties of surfactant systems. They investigated the damping rate of this wave and deduced the interfacial parameters. We have adopted a similar approach but with a completely different excitation scheme. We acoustically levitate a fluid drop in another immisible fluid and acoustically excite the drop into quadrupole oscillations (4,5,6).

The experimental setup is shown in Fig. 1. As suggested by Professor P.

Marston, the oscillation is detected by passing a parallel light beam through the drop, and collecting the scattered light by a photo-diode situated at the focal point of a lens. Since the wavelength of light is much smaller than the size of the drop, the scattering cross section is proportional to the geometrical cross section of the drop in the direction of the light beam. When the drop is oscillating, this cross section changes accordingly. A great advantage of this detection method is that the signal is not sensitive to the position of the drop as long as it is within the light beam. If the acoustical forcing is not continuous but an impulse, one can study the free oscillations of the drop. The signal received during free oscillation of the drop is digitized and stored in a computer. These data can be analyzed to obtain the free oscillation frequency and decay constant which are functions of the surface as well as bulk properties.

In order to relate the observed quantities to the unknown parameters, we have studied this problem theoretically. Generally the system is very complex if we attempt to include all properties in our model. Hence we examine a simpler system and concentrate on the more prominent effects of Gibbs elasticity by choosing surfactants exhibiting negligible surface viscosities on the interface. In our analysis, we assume that both fluids are incompressible and the process isothermal, and that the amplitude of the oscillation is much smaller than the wavelength along the surface. The last assumption allows us to neglect nonlinear terms in the equations. We use the normal mode analysis and perturbation method to solve the Navier-Stokes equations in spherical coordinates with the appropriate boundary conditions (7).

When the drop is oscillating, part of the surface is expanded and part of it is compressed. Therefore the surfactants are no longer evenly distributed on the surface. Moreover, due to the intrinsic coupling between the surface and bulk motions, the surfactant concentration in the bulk fluid is not homogeneous either. Thus, surfactant molecules will redistribute themselves in the bulk and on the surface through the diffusion and adsorption processes. Furthermore, there will be a surface tension gradient at the interface depending on the rate of the diffusion.

As shown in the Appendix, Gibbs elasticity E occurs naturally in the formulations, where E is $\partial\sigma/\partial\ln\Gamma$, σ is the interfacial tension, and Γ is the surface concentration of surfactants. The Gibbs elasticity is incorporated into the equations of the total stress balance. Together with the usual continuity of velocities and kinematic boundary condition, a general dispersion relation is derived. We have used Muller's method (8) to solve for the roots of the transcendental equation which yields the oscillation frequency and damping constant. Unfortunately, the results are very sensitive to the initial guess.

Thus, the numerical scheme needs to be improved. We have found, however, that to lowest order, the oscillation frequency decreases as the Gibbs elasticity increases for an insoluble film. This can be explained by noting that the interfacial tension gradient adds a new restoring force in the direction opposite to that due to the interfacial tension at the interface.

References

1. M. J. Boussinesq, Ann. Chim. Phys. 29 (1913) 349.
2. J. W. Gibbs, Trans. Connecticut Acad. 3, 108 (1878) 343.
3. L. Ting, D. Wasan, and K. Miyano, J. Colloid Interface Sci. 107 (1985) 345.
4. P. L. Marston and R. E. Apfel, J. Acoust. Soc. Am. 67 (1980) 27.
5. P. L. Marston, J. Acoust. Soc. Am. 67 (1980) 15.
6. C. J. Hsu and R. E. Apfel, J. Colloid Interface Sci. 107 (1985) 467.
7. C. A. Miller and L. E. Scriven, J. Fluid Mech. 32 (1968) 417.
8. K. E. Atkinson, An Introduction to Numerical Analysis (1978) 85.

B. Acoustic Nonlinear Parameter Determination

A method of accurately and reliably determining the Acoustic Nonlinear Parameter B/A in different liquids, semi-solids, and mixtures is necessary to characterize important features of these materials. Since B/A is a measure of the deviation of the pressure-density relationship from linear, it can provide valuable information about the nonlinear mechanical properties of materials and the propagation of waves through them (including waveform distortion, harmonic generation, changes in sound speed with pressure, etc.). For instance, characterization of human tissues by imaging of the Nonlinear Parameter *in vivo* may help doctors to discover and identify cancer tumors (the value of B/A is often different for healthy and malignant tissue; see Sehgal et al, J. Acoust. Soc. Am., 76(4), Oct. 1984). Moreover, a methodology has been proposed (J. Acoust. Soc. Am. 79(1), Jan. 1986) for predicting the composition of tissues from measurements of the density, sound velocity, and B/A using simple mixture laws. It may be possible to extend this methodology to determine the composition of other materials such as emulsions, polymers and rubber mixtures.

Previous investigators have used a variety of thermodynamic and finite amplitude techniques to measure B/A, which is defined by:

$$B/A = 2\rho_o c_o \left(\frac{\partial c}{\partial p}\right)_s = 2\rho_o c_o \left(\frac{\partial c}{\partial p}\right)_T + \frac{2c_o \beta T}{\rho_o C_p} \left(\frac{\partial c}{\partial T}\right)_p$$

We use a modified thermodynamic technique in which a rapid adiabatic (isentropic) pressure change of less than two atmospheres is produced, and the sound speed c is measured by acoustic interferometry. The apparatus is shown in Fig. 2. An electronic valve is opened via computer control, pressurizing the measurement cell at a rate sufficiently fast for an adiabatic process (time constant set by constriction valve). As pressure in the cell changes, the effective acoustic path length between the two ultrasound (5 MHz) transducers changes. The interferometer tracks the frequency necessary to maintain the same phase relationship between the transmitted and received signals (phase quadrature), which is proportional to the instantaneous sound speed. The frequency, the instantaneous pressure, and the instantaneous temperature are monitored by the computer which uses this information to calculate B/A. Since the experiment is computer-controlled, it is possible to make a large number of accurate and repeatable measurements upon which statistical analysis can be performed to further increase measurement precision.

During the past year, the system described above was assembled, debugged and tested. Preliminary data suggest that the value of B/A may be measured to a precision of less than 1%. This is comparable to that of the traditional thermodynamic techniques which require much greater variations in pressure and temperature (1 to 100 atm, 0 to 30 °C). Such extremes may render these techniques unsuitable for measuring the nonlinear parameter of certain substances (e.g. tissues) which may be adversely affected by them. The relatively modest pressure changes used in our technique, however, should not provide the same drawback. Moreover, in order to implement and test the mixture rules methodology described above, it is necessary to have accurate values of B/A for both mixtures and their components. Our technique provides us with the ability to make such measurements.

We acknowledge the support of the National Institutes of Health for the biological aspects of this project. We also acknowledge the support of the Office of Naval Research for the project's applications to non-biological materials of interest.

C. Microparticle Characterization Using Acoustic Scattering

The task of performing rapid and quantitative microparticle analysis has attracted considerable attention in a number or areas. Biological applications for cell characterization and separation technologies are numerous, due to the fact that changes in the optical and/or mechanical properties of biological cells often indicate disease. The measurement of particle size distributions in two phase flows is of considerable interest to those working in areas as diverse as combustion research, aerosol generation, cavitation, flow noise control, crude oil extraction, physical oceanography, and process control (to name a few).

By "characterization", we refer to the determination of one or more of the physical properties associated with a population of microparticles, be they geometrical (volume,shape), optical (index of refraction, fluorescence), or mechanical (density, elasticity). Which properties are significant depends on the specific application. A number of techniques exists for microparticle characterization. The various ensemble techniques, which include centrifugation, sound velocity and attenuation measurements, integrated light scattering and light extinction measurements (among others), are generally straightforward and non-invasive.

Single particle measurements generate more complete statistical information than ensemble observations, which yield only average values of physical properties over the entire population of particles. Electrical sensing zone instruments, which can measure the volumes of individual particles, cannot determine mechanical properties and are not well suited to *in situ* conditions. Single particle optical scattering techniques are sensitive and potentially non-invasive. They are, however, insensitive to mechanical properties and require optical access as well as sophisticated instrumentation and analysis.

To our knowledge, no technique exists for determining the mechanical properties of large numbers of individual microparticles. We have been working to develop such a characterization technology based on the principles of long wavelength acoustic scattering off of individual scatterers. This technique brings the advantages of single particle observations to the measurement of compressibility and density. We are able to distinguish populations within a sample and have the opportunity for selective particle sorting. The primary support for this work comes from the National Institutes of Health, which is concerned with the characterization of biological particles.

The basic theoretical problem is to determine the compressibility and density of a

fluid particle via the farfield scattering of incident plane acoustic waves. Invertible theories exist, most notably that attributed to Rayleigh, but they suffer from a stringent long-wavelength requirement: $ka<<1$, where "k" is the wave number and "a" is the radius of the scatterer. Also, the scattering pressure amplitude goes as the square of the frequency, which limits our sensitivity at long wavelengths. Thus, in applications in which the particle contrast is low (i.e. biological particles), we are limited by the Rayleigh theory to operating over a particle diameter range of about 1 to 5 micrometers (at 30 MHz).

Thus inspired, we have made some progress in developing simple and invertible weak scattering (Born) approximations, where we pose the scattering problem in its integral form and assume that the wave internal to the scatterer is simply related to the incident plane wave. It appears that we will be able to characterize weak scatterers over a size range such that $ka \leq 1$, a threefold improvement over the Rayleigh theory. We do so by measuring the farfield scattering at two angles (90° and 180°). This information, along with *a priori* knowledge of the particle size, permits us to determine the compressibility and density of individual particles. Conversely, we can determine the particle size given knowledge of either its compressibility or density. In the case of strong scatterers, such as gas bubbles, sensitivity is not an issue and the long-wavelength theory suffices.

Figure 3 shows a simplified block diagram of the scattering apparatus. Particles are convected by a coaxial jet flow through the focal region of two confocally positioned, focussed transducers, and into a sink where they can be recovered or discarded. The matched, high-Q transducers have a 30 MHz resonance frequency and a 1" focal length and the entire system is immersed in an appropriate host fluid (not necessarily transparent). One transducer produces 2 μsec long tone bursts of 30 MHz center frequency which scatter off of the particles as they individually flow through the focal zone. The same transducer detects the backscattered signal which is amplitude demodulated, peak detected, and stored on a DEC LSI 11/23 computer. The 90° signal is detected by the second transducer and processed in an identical manner.

Several problems (i.e. noise and sensitivity) associated with the transmit/receive switch and signal demodulator have been overcome in the past year, primarily through careful circuit design and construction. All of the signal demodulation and peak detection is done by analog hardware; thus high sampling rates (and correspondingly large jet flow rates) are attainable. At present, the computer restricts us to a sampling rate of 5 KHz, but this is not an inherent limitation.

Representative data is given in Figure 4, where the horizontal axis is time and the vertical axis corresponds to the scattered signal amplitude. This data was taken with 5 μm uniform polystyrene spheres. Each peak is the result of a single particle scattering about 8 echoes as it traverses the focal region. The shape of the peak is due to the roughly Gaussian transducer beam profile. Once the maxima of these peaks are determined, the properties of each particle can be calculated given knowledge of the particle size. We shall use polystyrene spheres as calibration particles.

The requirement of *a priori* knowledge of the particle size is a significant limitation. To deal with this, we plan to introduce a "coulter type" electrical sensing zone orifice at the tip of the jet nozzle. Such a device will provide us with individual particle size information. We can also use the orifice signal to gate both the computer and the sound field, so that we are generating and processing acoustical signals only while a particle is in the acoustic focus. This modification will permit us to increase substantially the total number of particles we can process with the computer and reduce the detrimental effects (jet deflection and broadening) brought on by acoustic streaming. Another feature of the "coulter" modified apparatus will be the potential for particle sorting. The principle signal processing is done in hardware, thus the scattering information is instantaneously available and can be combined with the orifice signal (via an appropriate decision criterion) to initiate selective downstream sorting.

There are several features that make this device useful and versatile. Particles are suspended in a host fluid; thus the particle shape is not distorted by any flat surfaces. We have the ability to distinguish populations within a sample of particles and determine the statistics of the mechanical properties. Since the scattered signal depends on the scatterer size via the nondimensional Helmholtz number (ka), the frequency of the device can be scaled in such a way as to permit observations over a broad range of particle sizes.

Even in applications where either the long-wavelength or the weak scattering theories don't apply, we can still detect and distinguish particles for purposes of counting, sorting, or monitoring. A small strong scatterer and a large weak scatterer are distinguished by simply evaluating the ratio of the 180° and the 90° signals. This ratio is approximately unity for gas bubbles and somewhat greater for fluid scatterers, a fact that would prove useful in an application such as *in situ* micro-bubble sizing in ocean water. In a similar fashion, we can discriminate solid and fluid particles, which makes this technology useful for various types of process control and machine status monitoring (e.g. detection of solid wear particles in engine lubricating oil).

The technology is inexpensive and robust and the theory is simple but limited. Applications exist wherever the detection, discrimination, or characterization of microparticles based on mechanical properties or size is required.

D. Stealth Acoustics

Calibration of transducers using scattering from, or radiation pressure on, spheres and cylinders is a common practice in Navy and other laboratories. In the last year we investigated the possibility of a unique calibration technique for high frequency (1-5 MHz) transducers. Our scheme involved acoustically levitating a 1 mm oil drop in water, using a small standing wave cell, and then using the transducer to be calibrated to displace the drop from its equilibrium levitated position by forces due to radiation pressure. The levitation signal was then increased to draw the drop to its initial levitated position. This nulling technique, along with an expression for the acoustic radiation pressure on the sphere, would then allow us to calculate the strength of transducer signal at the position of the drop.

The problem we faced was simply that the values of ka ($=2\pi fa/c$), where f is the frequency of the transducer to be calibrated, were above one (about eight in our experiments), and in this range the scattering Force Function varies rapidly with size and frequency. A small error in size measurement could lead to a large error in the predicted transducer sensitivity. An example of the calculated Force Function for our case is given in Figure 5a.

How could we smooth out this variation so that transducer strength could be measured precisely?

One observation was made quickly. For spheres for which the sound velocity of the drop, c*, is greater than that in the surrounding host medium, c, (as it is with solid spheres), the variations of the Force Function are much less, primarily because parallel rays incident on the sphere refract away from the sphere's centerline rather than toward it. Interference effects between incident rays and multiply refracted rays are less in this case. (Waves that creep around the sphere are, however, present in this case.)

In our calibration technique, this arrangement was not possible, because the drop being levitated must be sufficiently *more* compressible than the surrounding medium, and that means, for practical liquids, that the sound velocity of the drop must be *less* than the host sound velocity.

But all was not lost. I suggested that perhaps if we were to match impedances ($\rho^*c^* = \rho c$), keeping $c^* < c$, as required for levitation, and compensating by making $\rho^* > \rho$, then perhaps we could postpone the rapid variations of the Force Function to higher ka. The results for a 10% and 20% discrepancy between c* and c are shown in

Figures 5b and 5c.

The remarkable result of a smooth Force Function up to much higher ka in Figures 5b and 3c is attributed to the following: Rays approaching along the centerline are not refracted. Since the impedance is matched, these rays go through without reflection. Rays off center are both transmitted and reflected, but the closer to the centerline, the weaker the return signal. The farther away from the centerline, the more energy is reflected back, but before a ray can come back parallel to the incident ray (and interfere with it), it must undergo many internal reflections. Therefore, interference effects are feeble at low ka.

The consequences of these observations are both good and bad. They are bad for our calibration experiment, because the matched impedance condition means a much stronger levitation signal is required, to the point where acoustic cavitation occurs.

The good consequence may be that it appears that we may be able to tailor targets so that an acoustical probing signal is not successful in determining the signature of the target (shape, size, and material properties). We do this by using materials and coatings that match impedance while not requiring that $\rho = \rho^*$, $c = c^*$.

Matching impedances is, of course, not a new idea. But this strategy is strictly true for objects for which the relevant size scales are very large compared to a wavelength. Our analysis suggests the ability of impedance matching when the size scales are comparable to an acoustic wavelength. It remains to be seen whether this approach to "stealth" acoustics is either novel or useful.

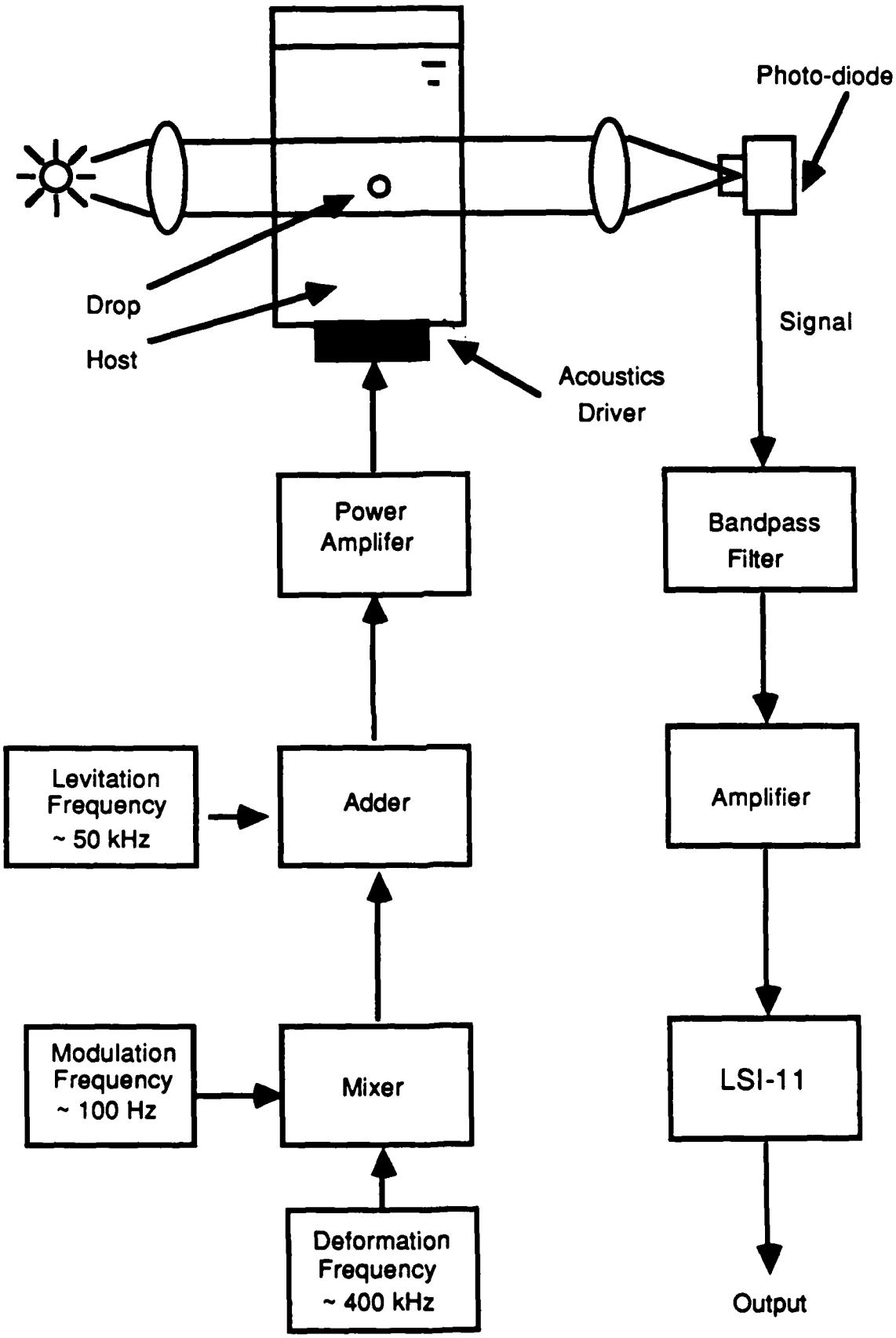

Figure 1: Experimental Setup for Interfacial Characterization

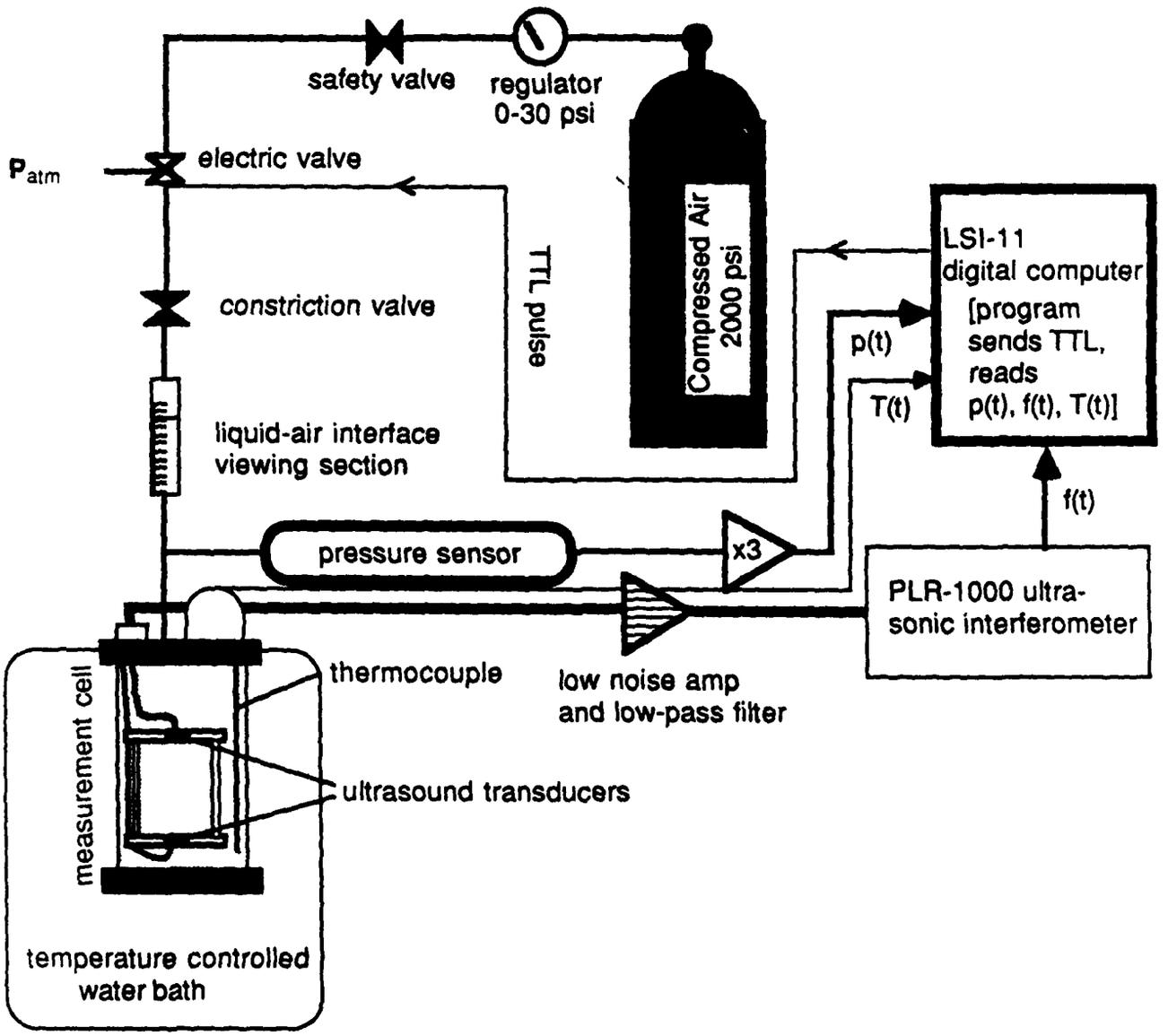

Figure 2: B/A EXPERIMENTAL APPARATUS

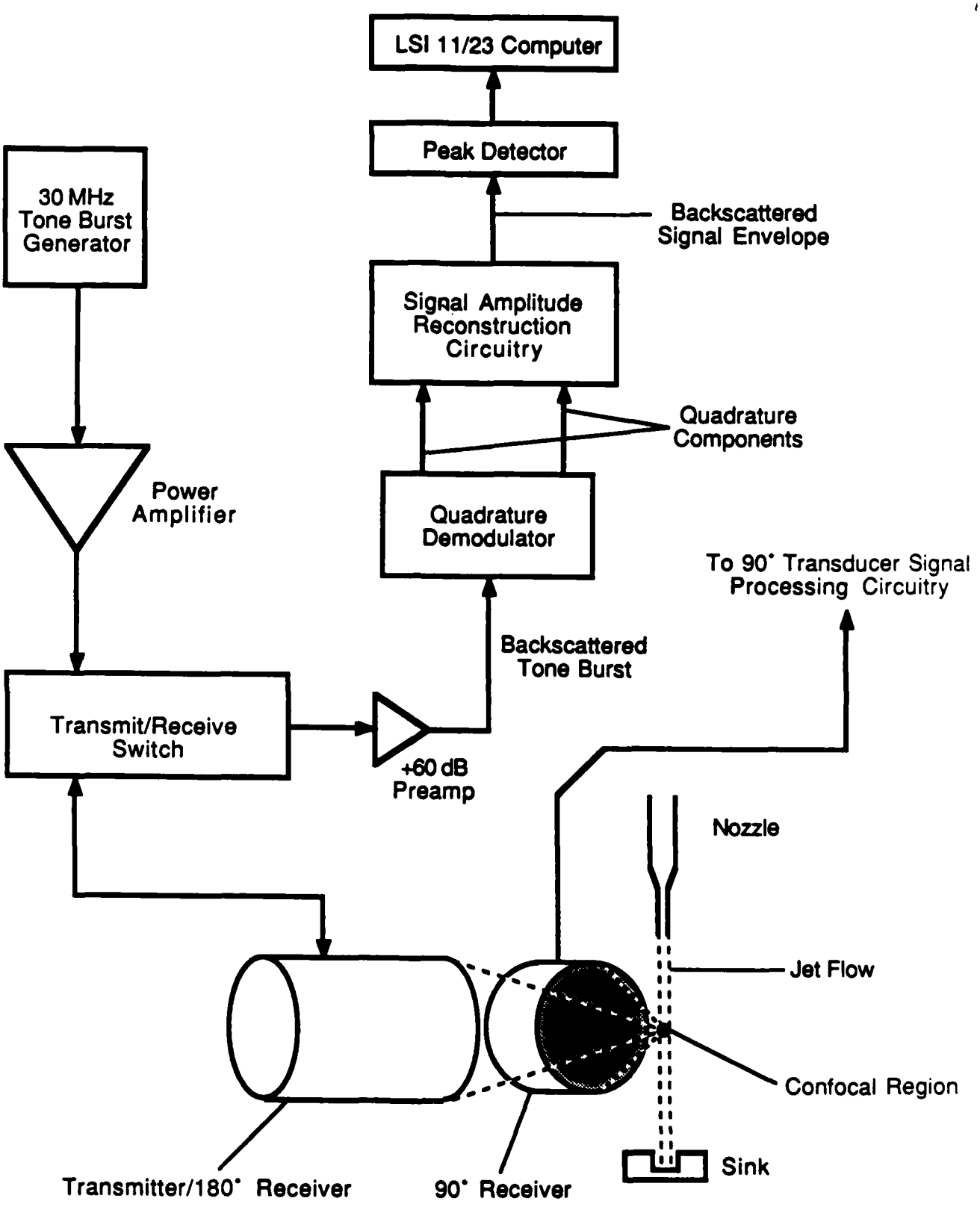

Figure 3: Block Diagram of the Microparticle Characterization Apparatus (180° channel only)

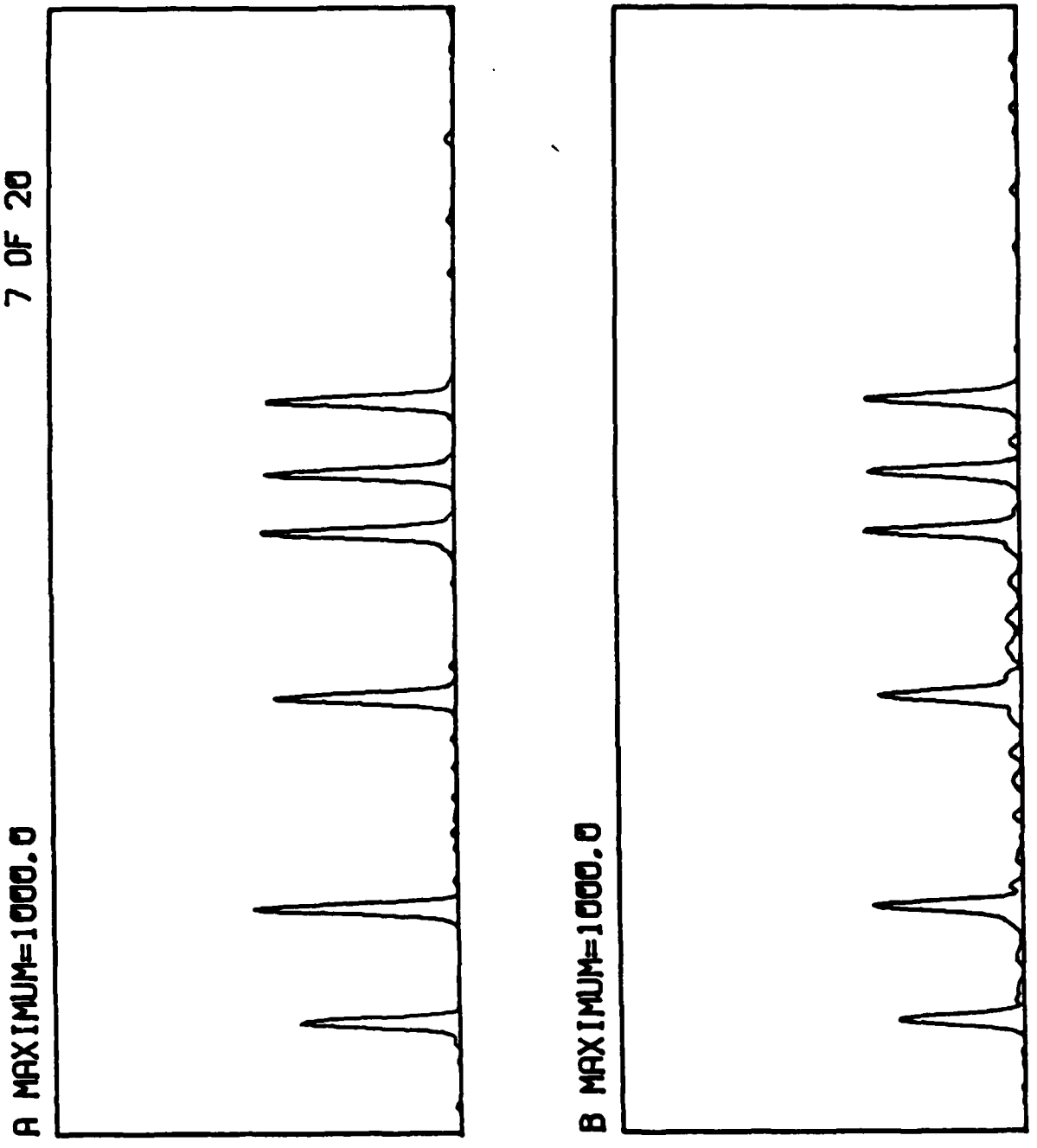

Figure 4: Representative Microparticle Data

Figure 5: FORCE ON A FLUID SPHERE AS A FUNCTION OF KA

5A:

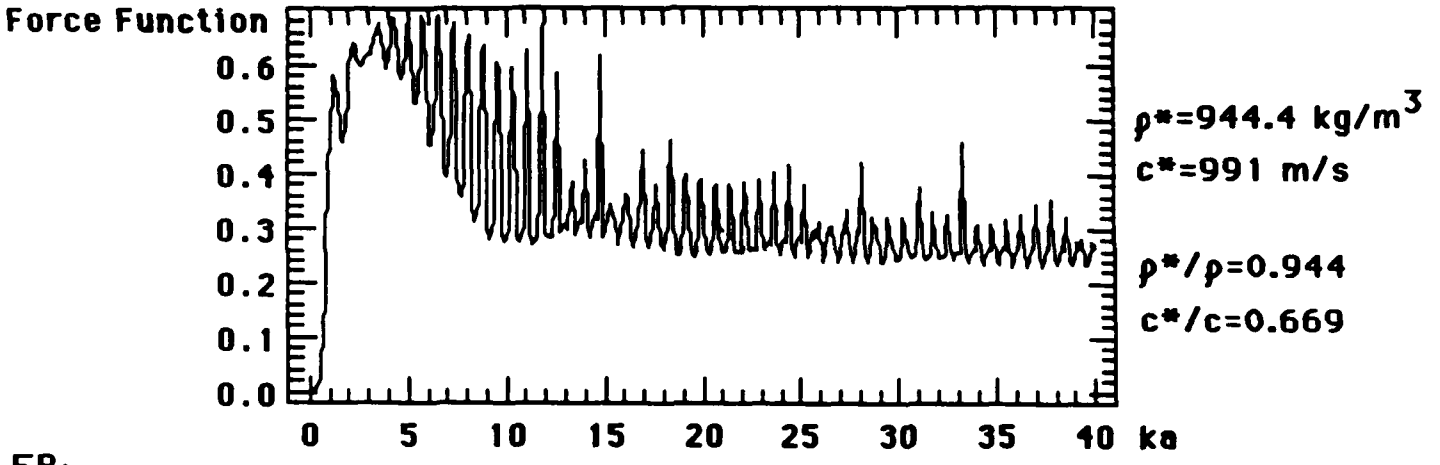

5B:

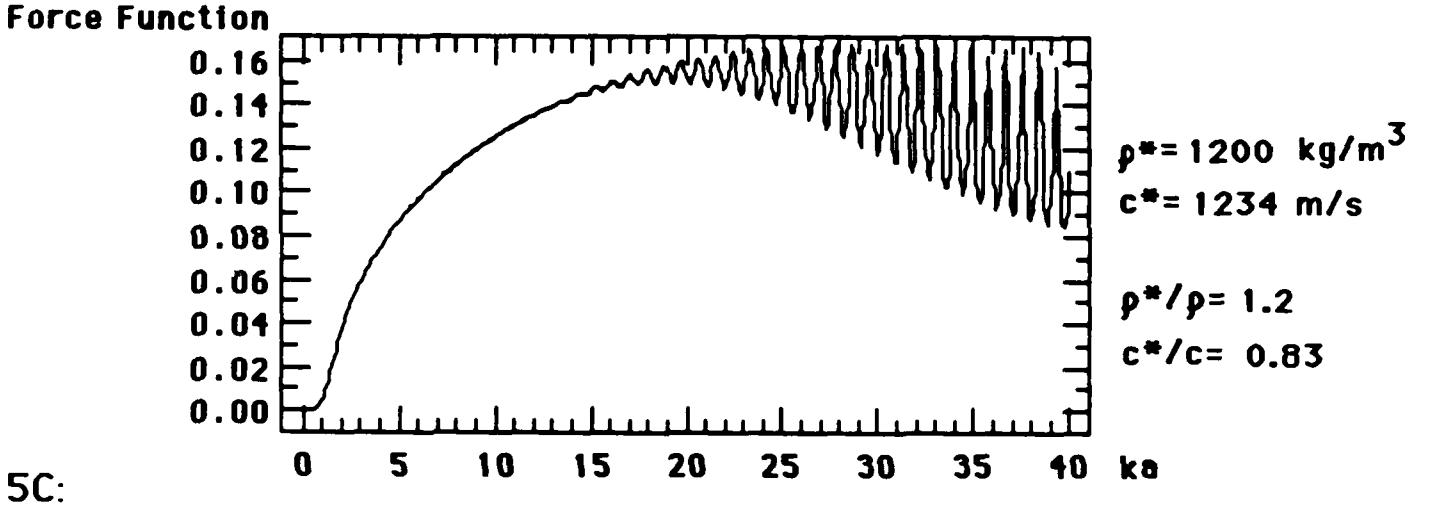

5C:

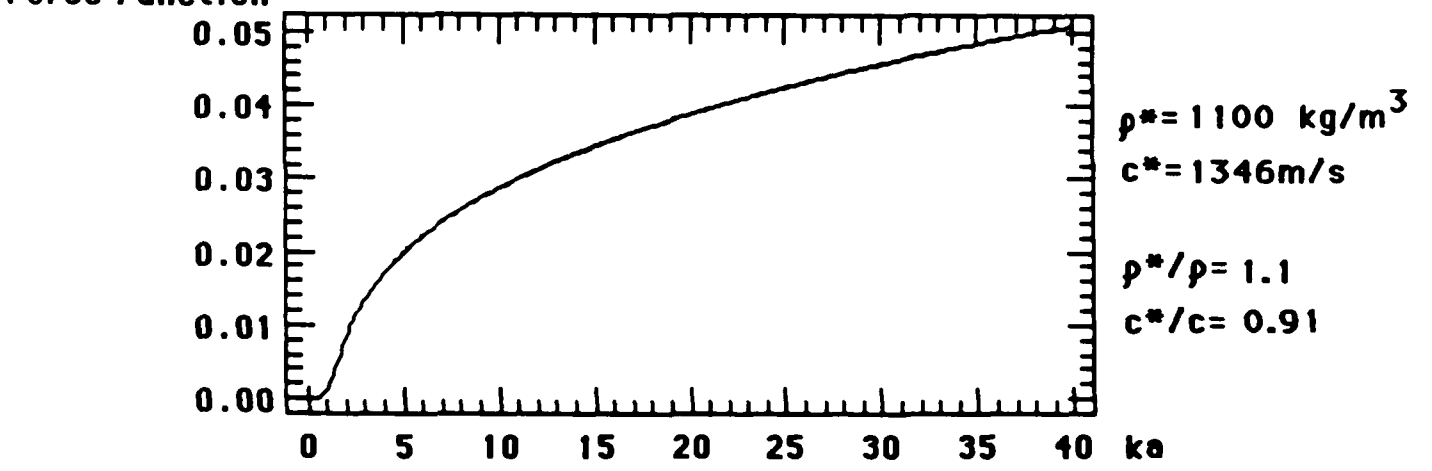

Appendix

The Surface Tension Variations with the Surfactant Concentrations

For simplicity, the case of a liquid drop oscillating in air is considered below. The calculations for the more general case, a liquid drop oscillating in another liquid, is performed in the same way.

The drop has density ρ, surface tension σ, kinematic viscosity ν, and radius R. The bulk surfactant concentration is C, and the surface concentration is Γ. The diffusion constant of the surfactant in the bulk is D, and is D_s on the surface. In the bulk, the fluid satisfies

$$\vec{\nabla} \cdot \vec{v} = 0 \qquad \text{--- (A1)}$$

$$\frac{\partial \vec{v}}{\partial t} = - \frac{1}{\rho} \vec{\nabla} p + \nu \nabla^2 \vec{v} \qquad \text{--- (A2)}$$

where $\vec{v}$ is the velocity field, and p is the pressure field. Nondimensionalize A(1) and A(2) by changing

$$t \rightarrow \frac{t}{\omega_\alpha} \ , \quad p \rightarrow \rho \, \omega_\alpha^2 R^2 p \ , \quad \vec{v} \rightarrow R \, \omega_\alpha \vec{v} \ , \quad r \rightarrow r R ,$$

then (A1) and (A2) become

$$\vec{\nabla} \cdot \vec{v} = 0 \qquad \text{--- (A3)}$$

$$x^2 \frac{\partial \vec{v}}{\partial t} = - x^2 \vec{\nabla} p + \nabla^2 \vec{v} \quad , \text{ where } \quad x^2 = \frac{R^2 \omega_\alpha}{\nu} \qquad \text{--- (A4)}$$

ω_α denotes the oscillation frequency of the drop in the mode α. (A3), (A4) can be solved by the standard method in terms of the spherical Bessel function (j_α) and the spherical

harmonics ($Y_{\alpha\beta}$). Because of the intrinsic coupling between the surface and bulk motions, the surfactant molecules will redistribute themselves in the bulk and on the surface. The motions of the surfactants are governed by

$$\frac{\partial C}{\partial t} + \vec{\nabla} \cdot C\vec{\nabla} = D\nabla^2 C \qquad \text{--- (A5)}$$

$$\frac{\partial \Gamma}{\partial t} + \vec{\nabla}_s \cdot \Gamma \vec{\nabla}_s = D_s \nabla_s^2 \Gamma + D \left(\frac{\partial C}{\partial n}\right)_s \qquad \text{--- (A6)}$$

(A6) is served as a boundary condition of (A5). Again, linearize and nondimensionalize (A5) and (A6) by changing

$$C \to C_0 C \ , \quad \Gamma \to \Gamma_0 \Gamma, \ t \to t/\omega_\alpha \ , \quad \vec{\nabla} \to \vec{\nabla}/R \ , \qquad \text{and using}$$

$$\frac{\partial \Gamma}{\partial t} = \frac{\Lambda}{C_0}\frac{\partial C}{\partial t} \ , \qquad \nabla_s^2 \Gamma = \frac{\Lambda}{C_0}\nabla_s^2 C$$

$$\Lambda = \left(\frac{\partial \Gamma}{\partial \ln C}\right)_0 , \qquad \left(\frac{\partial C}{\partial n}\right)_s = \left(\frac{\partial C}{\partial r}\right)_s$$

Then (A5) and (A6) become

$$\nabla^2 C + y^2 C = 0, \qquad \text{where} \quad y^2 = \omega_\alpha R^2/D \qquad \text{--- (A7)}$$

$$\frac{\Lambda}{\Gamma_0}\left(z^2\frac{\partial C}{\partial t} - \nabla_s^2 C\right)_s + z^2 \vec{\nabla}_s \cdot \vec{\nabla}_s = \frac{D C_0 R}{\Gamma_0 D_s}\left(\frac{\partial C}{\partial r}\right)_s \qquad \text{--- (A8)}$$

$$\text{where,} \qquad z^2 = \frac{\omega_\alpha R^2}{D_s}$$

The variables with subscript s should be evaluated on the surface. Λ is the parameter which describes the adsorption of the surfactants on the surface. The solution of (A7) is

$$C = C_{\alpha\beta} j_\alpha(yr)\, Y_{\alpha\beta}\, e^{-t} \qquad , \text{ where}$$

$$C_{\alpha\beta} = \frac{-\alpha(\alpha+1)\left(a_i((\alpha+1) j_\alpha(x) - x j_{\alpha+1}(x)) + P_i \right)}{\frac{\Lambda}{\Gamma_0}\left(1 - \frac{\alpha(\alpha+1)}{z^2}\right) j_\alpha(y) + \frac{D C_0 R}{\Gamma_0 D_s z^2}\left(\alpha j_\alpha(y) - y j_{\alpha+1}(y)\right)}$$

The a_i and p_i are the same coefficients which appear in the solution of V_r.

$$V_r = \frac{\alpha(\alpha+1)}{r^2}\left(a_i r j_\alpha(xr) + \frac{p_i r^{(\alpha+1)}}{(\alpha+1)} \right) Y_{\alpha\beta}\, e^{-t}$$

If the variation of the surfactant concentration is small, the surface tension can be expanded in terms of C to first order at the equilibrium point where the bulk concentration is C_0 and surface concentration is Γ_0.

$$\sigma = \sigma_0 - E\Lambda C$$

$$= \sigma_0 - -\frac{E\Lambda}{\Gamma_0} C_{\alpha\beta} j_\alpha(x)\, Y_{\alpha\beta}\, e^{-t} \qquad \text{, where } E = -\left(\frac{\partial\sigma}{\partial \ln \Gamma}\right)_0$$

If D and D_s are very small, i.e. $D, D_s << 1$,

$$\sigma = \sigma_0\left(1 - \alpha(\alpha+1)\frac{E}{\sigma_0}\left(a_i((\alpha+1) j_\alpha(x) - x j_{\alpha+1}(x)) + P_i \right) Y_{\alpha\beta}\, e^{-t}\right)$$

For $z >> 1$, it is true generally,

$$\sigma = \sigma_0 \left(1 - \alpha(\alpha+1)\frac{E}{\sigma_0} \left(a_i((\alpha+1) j_\alpha(x) - x j_{\alpha+1}(x)) + P_i \right) \cdot \right.$$

$$\left. \left(1 + \frac{\alpha(\alpha+1)}{z^2} - \frac{D C_0 R}{\Gamma_0 \Lambda z^2} \left(\alpha - y \frac{j_{\alpha+1}(y)}{j_\alpha(y)} \right) \right) Y_{\alpha\beta} e^{-t} \right)$$

The surface tension variation with the surfactant concentration is incorporated into the stress balance equations which are

$$T_{rr} = 2 \sigma H$$

$$\vec{T}_s = \vec{\nabla}_s \sigma$$

T_{rr} is the net radial stress, and $\vec{T}_s$ is the net tangential stress.

II. Manuscripts Published or Submitted for Publication

R. E. Apfel, "Whispering Waves in a Wineglass," Am. J. Phys. 53,1070(1985).

C. J. Hsu and R. E. Apfel, "Model for the Quadrupole Oscillation of Drops for Determining Interfacial Tension," J. Acoust. Soc. Am.---in review.

M. S. Roos, S. C.Wardlaw, and R. E. Apfel, "Application of 30 MHz Acoustic Scattering to the Study of Human Red Blood Cells----Submitted for Publication

R. E. Apfel, "Prediction of Tissue Composition from Ultrasonic Measurements and Mixture Rules," J. Acoust. Soc. Am. 79, 148(1986).

R. E. Apfel, "Possibility of Microcavitation from Diagnostic Ultrasound," IEEE UFFC-33, 139(1986).

Zhe-ming Zhu and R. E. Apfel, "Shape Oscillations of Microparticles on an Optical Microscope Stage," J. Acoust. Soc. Am. 78, 1796(1985).

END

3-87

DTIC